PCCP

View Online
Dynamic Article Links

Cite this: *Phys. Chem. Chem. Phys.*, 2011, **13**, 5462–5471

www.rsc.org/pccp

PAPER

Methylene blue and neutral red electropolymerisation on AuQCM and on modified AuQCM electrodes: an electrochemical and gravimetric study†

Madalina M. Barsan, Edilson M. Pinto and Christopher M. A. Brett*

Received 17th February 2011, Accepted 22nd February 2011
DOI: 10.1039/c1cp20418a

The phenazine monomers neutral red (NR) and methylene blue (MB) have been electropolymerised on different quartz crystal microbalance (QCM) substrates: MB at AuQCM and nanostructured ultrathin sputtered carbon AuQCM (AuQCM/C), and NR on AuQCM and on layer-by-layer films of hyaluronic acid with myoglobin deposited on AuQCM (AuQCM-{HA/Mb}$_6$). The surface of the electrode substrates was characterised by atomic force microscopy (AFM), and the frequency changes during potential cycling electropolymerisation of the monomer were monitored by the QCM. The study investigates how the monomer chemical structure together with the electrode morphology and surface structure can influence the electropolymerisation process and the electrochemical properties of the phenazine-modified electrodes. Differences between MB and NR polymerisation, as well as between the different substrates were found. The electrochemical properties of the PNR-modified electrodes were analysed by cyclic voltammetry and electrochemical impedance spectroscopy and compared with the unmodified AuQCM. The results are valuable for future applications of modified AuQCM as substrates for electroactive polymer film deposition and applications in redox-mediated electrochemical sensors and biosensors.

1. Introduction

The electrochemical quartz crystal microbalance (EQCM) is a powerful tool that enables the simultaneous *in situ* monitoring of both mass changes and current during the potential cycling. The technique can be successfully employed to obtain information about the deposition of various types of films at the quartz crystals. The main limitation of piezoelectric quartz crystals for application in electrochemistry is the fact that they are based on metal film coatings, which are susceptible to forming surface oxides or to dissolving. This problem was overcome by developing sputtered carbon film gold QCM (AuQCM) electrodes and their improved electrochemical properties demonstrated that they are good candidates for the development and characterisation of electrochemical sensors and biosensors.[1] Other modified AuQCM electrodes, which showed viability for use in biosensors, were recently developed: hyaluronic acid and myoglobin layer-by-layer modified AuQCM electrodes.[2,3] This type of protein immobilisation allows the intercalation of very small amounts of compound in an ultrathin nano-ordered structure, without alteration of its initial conformation.

These two types of modified AuQCM together with unmodified AuQCM electrodes were used as substrates for the monitoring of the polymerisation of the phenazine monomers neutral red and methylene blue, with the aim of exploring firstly whether the newly developed modified AuQCM electrodes lead to better polymerisation of both monomers, and secondly if they are good candidates for biosensors. This class of phenazine polymer films has gained increasing interest due to the wide application of these polymers in sensor and biosensor devices, recently reviewed in ref. 4 within which poly(neutral red), PNR, and poly(methylene blue), PMB, are among the more often used.[5–8] Phenazine dyes are aromatic compounds with a dibenzo annulated azine structure and their derivatives have a methyl and/or amino group attached to the benzene rings and one N can be substituted by S (phenothiazine) as in the case of MB, see Fig. 1. The phenothiazine dye thionine sparked interest in the late 1970s and 1980s due to its possible application in photogalvanic cells,[9] which included investigations into the kinetics and mechanism at thionine-modified electrodes *e.g.* ref. 10.

Researchers have focused interest on investigating how counterions and protons are involved in the redox process of

Departamento de Química, Faculdade de Ciências e Tecnologia, Universidade de Coimbra, 3004-535 Coimbra, Portugal. E-mail: brett@ci.uc.pt; Fax: +351-239-835295; Tel: +351-239-835295

† This article is part of the special collection on *Interfacial processes and mechanisms* in celebration of John Albery's 75th birthday.

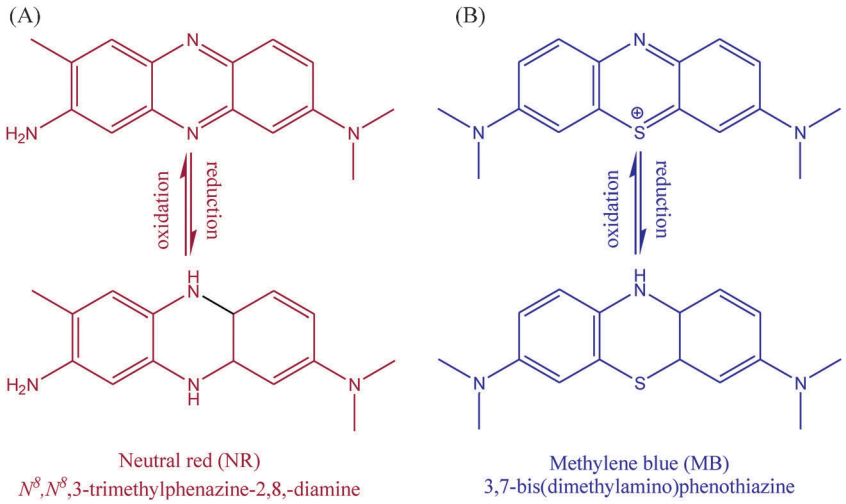

Fig. 1 Chemical structures of oxidised and reduced forms of (A) neutral red (NR) and (B) methylene blue (MB).

the phenazine polymer. Benito *et al.* reported an electrochemical impedance and ac-electrogravimetry study of PNR films and observed that the participation of hydronium ions during the electrochemical process is important in acidic media, while at higher pH, the participation of anions increases substantially and substitutes the hydronium ions.[11] In the case of PMB, many attempts have been made to clarify the deposition process of the electropolymerised film. Clavilier *et al.* reported, in a series of papers, an electrochemical examination of the adsorption of MB on thermally treated gold electrodes,[12–14] observing that the presence of a zero valent sulfur monolayer on the electrode surface enhanced the adsorption of MB due to a nonbonding S–S interaction. More recently, Kertész *et al.* described the simultaneous gravimetric and voltammetric monitoring of the formation and redox transformations of PMB films using EQCM;[15] they also investigated how the anion, cation and pH can influence the electrochemical process of the polymer.

The polymerisation process of phenazine monomers is complex, and is still unclear, as is the influence of the chemical structure of the monomers together with the morphological and structural characteristics of the substrates. This paper describes the electropolymerisation process by potential cycling of the monomers methylene blue (MB) and neutral red (NR) on different substrates based on gold piezoelectric quartz crystals (AuQCM) of different surface structures characterized by AFM, with simultaneous gravimetric monitoring. The electrochemical properties of PNR-modified electrodes were investigated by electrochemical impedance spectroscopy (EIS) and by cyclic voltammetry (CV).

2. Experimental

2.1 Reagents and buffer electrolyte solutions

The phenazine monomer methylene blue (MB) and the phenothiazine neutral red (NR), 65% dye content, were from Aldrich (Germany).

The buffer solution used for the electropolymerisation of MB was 0.025 M borate buffer ($Na_2B_4O_7$) with the addition of 0.1 M Na_2SO_4 (both from Merck, Germany) and for NR was 0.025 M potassium phosphate saline (KPBS) pH 5.5 prepared from KH_2PO_4 and K_2HPO_4 (Riedel-deHaën, Germany) with the addition of 0.1 M KNO_3 (Fluka, Switzerland), according to previously optimised procedures.[16,17] The concentration of the dyes dissolved in the buffer solutions was 1.0 mM.

The electrolyte used for the characterisation of the phenazine modified electrodes was 0.1 M KCl (Panreac, Spain).

Millipore Milli-Q nanopure water (resistivity $\geq$ 18 MΩ cm) and analytical reagents were used for the preparation of all solutions. Experiments were performed at room temperature, 25 $\pm$ 1 °C.

2.2 Electrodes and instrumentation

Electrochemical characterisation was carried out in a conventional electrochemical cell containing three electrodes, the AuQCM or surface-modified AuQCM electrode as working electrode, a platinum foil as counter electrode, and a saturated calomel electrode (SCE) as reference. The AuQCM electrodes were prepared from AT-cut piezoelectric quartz crystals (KVG Germany), 6 MHz with an exposed geometric area of 0.28 cm^2. Au electrodes were first cleaned with piranha solution (3 : 1 H_2SO_4 95–97%: H_2O_2 35%), then washed with Milli-Q water, and dried in a stream of pure N_2.

For AuQCM/C, thin carbon films of 500 nm thickness were deposited by rf magnetron sputtering (energy 1 keV) after washing the AuQCM metal substrates in 0.1 M perchloric acid. The target material was produced by heating graphitic carbon.[1] The layer-by-layer films, produced at pH 5.0 of hyaluronic acid (HA) in its anionic form with the myoglobin (Mb) with positively charged amine groups at this pH, were self-assembled on precursor-modified AuQCM electrodes, following the procedure described in ref. 2 and 3.

AFM was performed with a Multimode TM Atomic Force Microscope controlled by a Digital Instruments Nanoscope E controller (Veeco Instruments, USA). Silicon nitride NanoProbe TM V-shaped cantilevers, 100 nm length and 0.58 N m^{-1} spring constant were used. All images were recorded in non-contact mode AFM in air at room temperature.

Voltammetric measurements were performed by using a computer-controlled μ-Autolab Type II potentiostat-galvanostat running with GPES 4.9 for Windows software (Metrohm-Autolab, Utrecht, Netherlands).

EIS experiments were carried out by using a PC-controlled Solartron 1250 Frequency Response Analyzer, coupled to a Solartron 1286 Electrochemical Interface (Solartron Analytical, UK), using ZPlot 2.4 software (Scribner Associates Inc., USA) with an rms perturbation of 10 mV applied over the frequency range 65.5 kHz to 0.01 Hz, and 10 frequency values per frequency decade. The spectra were recorded at the open circuit potential (OCP), measured just before each EIS experiment, and at −0.35 and −0.48 V *vs.* SCE. The spectra were fitted to electrical equivalent circuits with ZView 3.2 software (Scribner Associates Inc., USA).

Gravimetric studies were performed by using a homemade electrochemical quartz crystal microbalance (EQCM), without the ability to record dissipation, connected to a μ-Autolab (Metrohm-Autolab, Netherlands), controlled by GPES 4.9 software. The mass/frequency correlation factor obtained for the system, according to the Sauerbrey equation[18] is 3.45 ng Hz^{-1} where $\Delta f = -2.91 \times 10^8 \Delta m$.

The pH-measurements were done with a CRISON 2001 micro pH-meter.

3. Results and discussion

3.1 AFM characterisation of AuQCM, AuQCM/C and AuQCM-{HA/Mb}$_6$ surfaces

Surface characterisation of the AuQCM, AuQCM/C and AuQCM-{HA/Mb}$_6$ substrates was made by AFM and the images obtained are presented in Fig. 2.

The unmodified AuQCM surface is the less rough, with homogeneously distributed gold nanostructures of a radius smaller than 50 nm (see Fig. 2(A)). The AuQCM covered by sputtered carbon, has a rougher surface, with carbon structures up to 80 nm in diameter, as can be seen in Fig. 2(B). Moreover, cavities and protrusions are formed during the deposition process of carbon films, as mentioned

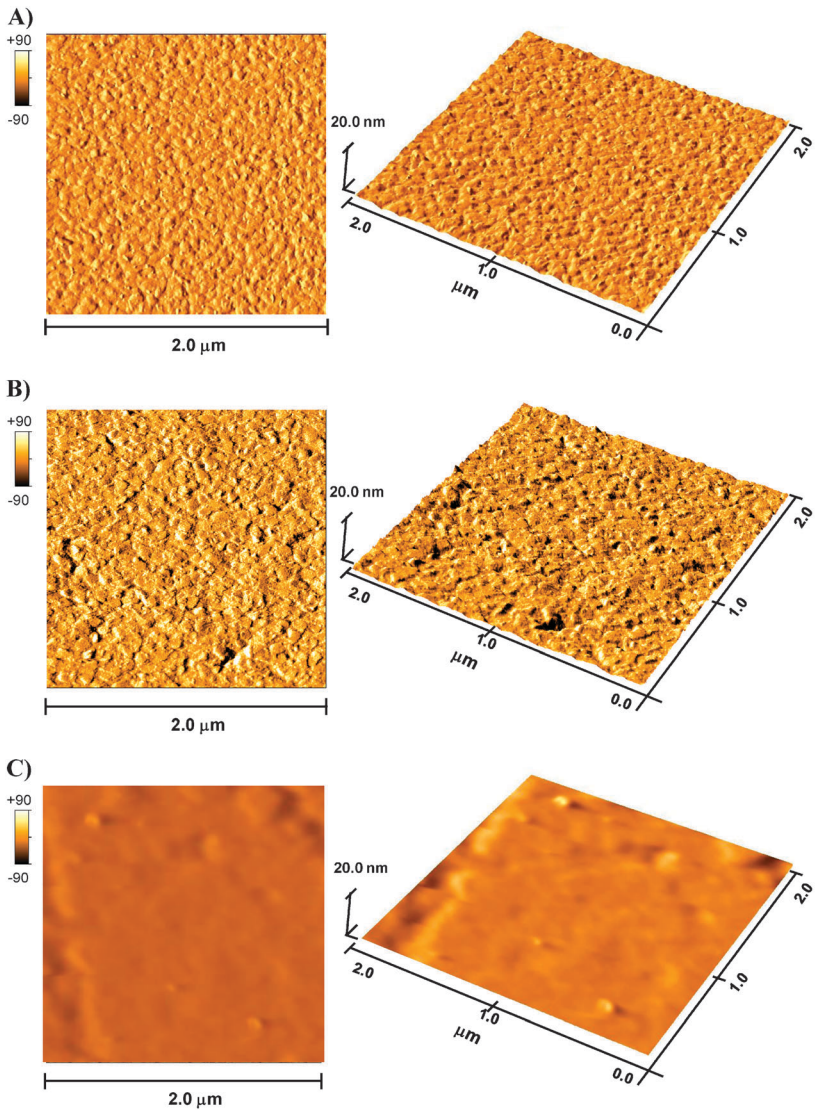

Fig. 2 AFM images of unmodified and modified AuQCM surfaces in 2D and 3D for (A) AuQCM, (B) AuQCM/C and (C) AuQCM-{HA/Mb}$_6$.

in previously published work.[1] The LBL modified AuQCM has a very smooth surface (Fig. 2(C)), as also observed in ref. 3.

The mean roughness, R_a, is defined as the absolute average deviation of the roughness irregularities from the mean line over one sampling length.[19] The calculated roughness parameter obtained for AuQCM was R_a = 1.25 nm, increasing to R_a = 1.32 nm for AuQCM/C and the lowest value of 0.95 nm for the LBL modified one.

The surface roughness of the substrate plays an important role in the polymerisation of the monomer dyes, principally in the monomer adsorption step which initiates the process, as will be presented below. Rougher surfaces have a larger surface area and, therefore, more nucleation sites are available for polymer growth.

3.2 Poly(methylene blue) deposition on AuQCM and AuQCM/C

The electropolymerisation of MB was carried out by cycling the potential between −0.65 V and +1.0 V *vs.* SCE at 50 mV s^{-1} in a solution containing 1 mM monomer in 0.025 M $Na_2B_4O_7$ + 0.1 M Na_2SO_4, pH 9.25. The chemical structure of both oxidised and reduced forms of monomer (corresponding to polymer as well) are presented in Fig. 1(B) and possible linkages between monomer moieties during polymerisation are shown schematically in Fig. 3. Cyclic voltammograms recorded during the electropolymerisation are presented in Fig. 4(A) and (B). In the case of the AuQCM substrate, 40 cycles were needed to complete the electropolymerisation, since after this no increase in the current was observed. At AuQCM/C electrodes the CVs stabilised after 30 cycles, the process being faster in this case.

As for all phenazine-type monomers, the electropolymerisation process begins with the adsorption of monomer at the electrode surface and, since the AuQCM and AuQCM/C surface is hydrophobic, the monomer, which is also hydrophobic due to its condensed aromatic structure, will be adsorbed with the three linked hydrophobic rings parallel to the electrode surface.[20,21] The first pair of peaks presented in Fig. 4(A) and (B) are attributed to the monomer, and are also recorded if the potential is cycled at +0.4 V *vs.* SCE, before radical cation formation. If the potential is cycled at +1.0 V, as shown in Fig. 4, an irreversible oxidation peak appears at positive potentials close to +1.0 V *vs.* SCE, more evident in Fig. 4(B). The fact that it is an irreversible oxidation indicates the formation of radical species, which then react with other monomers, initiating polymerisation. This is also explained by the appearance of the second pair of peaks after a few potential cycles, shifted towards more positive potentials, and which is attributed to the polymer formed on the electrode surface. This kind of CV profile is also reported for other phenoxazines and phenothiazines, such as brilliant cresyl blue,[22] methylene green,[16] Meldola blue,[20] Nile blue and toluidine blue.[23]

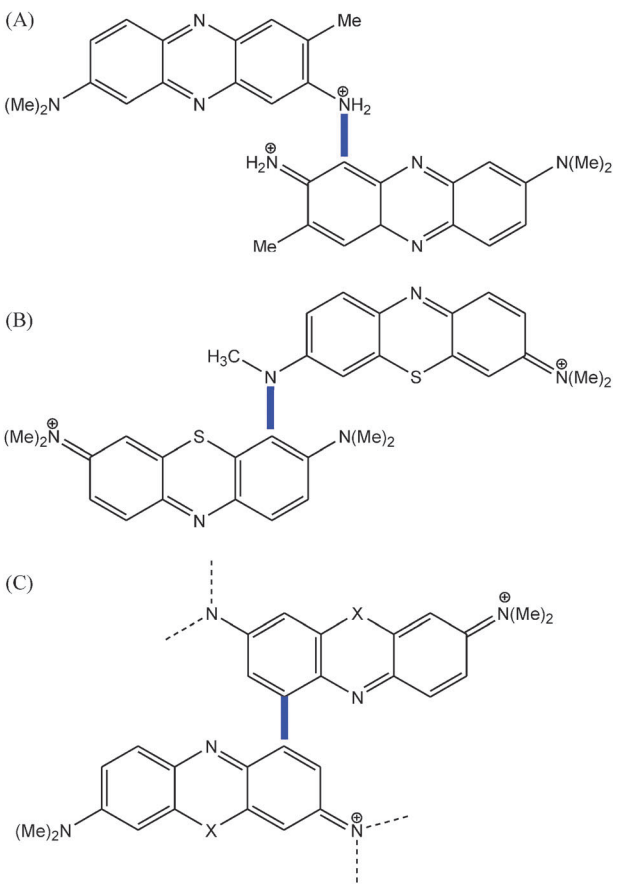

Fig. 3 Possible chemical linkage of NR and MB monomers during polymerisation: (A) primary amine-ring linkage for NR; (B) tertiary amine-ring linkage for MB and (C) ring to ring binding for both NR and MB.

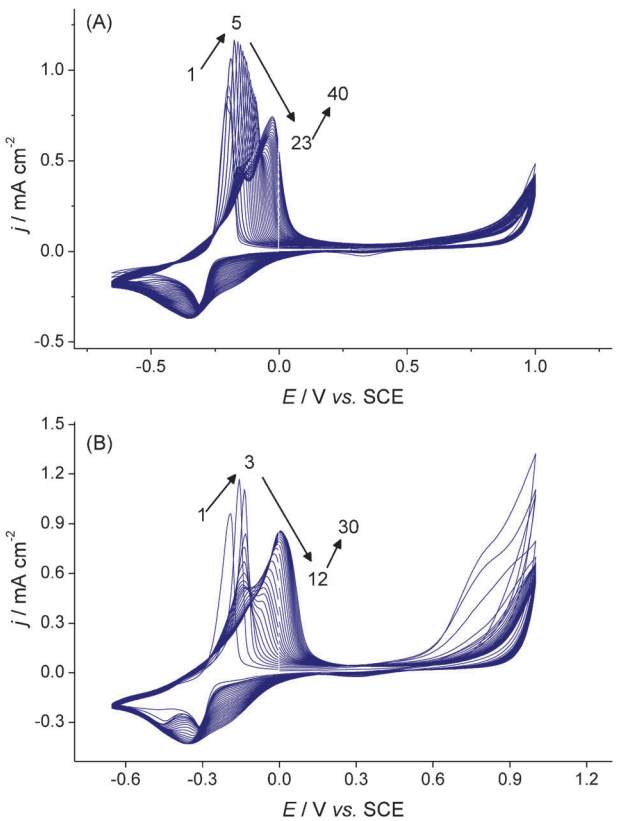

Fig. 4 CVs recorded during the electropolymerisation of MB at (A) AuQCM and (B) AuQCM/C from a solution containing 1 mM MB in 0.025 M $Na_2B_4O_7$ + 0.1 M Na_2SO_4 pH 9.25; v = 50 mV s^{-1}.

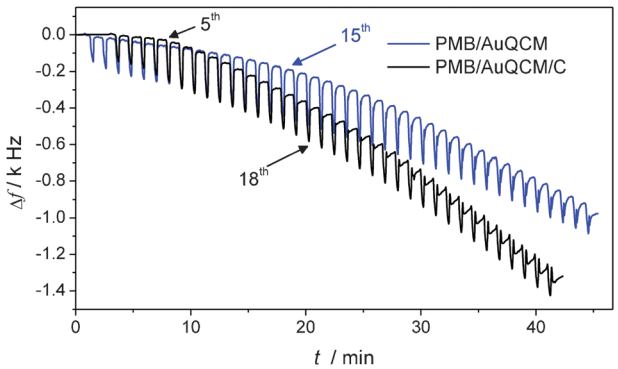

Fig. 5 Frequency shift recorded during the electropolymerisation of MB on AuQCM and AuQCM/C substrates.

When monomers contain two tertiary amino groups, which is the case for MB, the oxidation potential of the monomer which results in the formation of the cation radical is more positive than for monomers which contain a primary amino group (–NR), being closer to the oxygen evolution region. A higher energy is required for the formation of the radical cation when only tertiary amino groups are present as ring substituents; the irreversible oxidation of the MB involves the oxidation of a methyl group attached to one of the tertiary amino groups, which is oxidised to formaldehyde.[21] The very unstable radical cation formed links to the aromatic ring of another monomer molecule, adjacent to an $-NH_2$ group, since this carbon atom is more electronegative (see Fig. 3(A)). In both cases, for NR and MB, besides the "head to tail" linkage *via* an amino group, there is the possibility of "ring to ring" binding, as shown in Fig. 3(C). In this case, the more electronegative aromatic carbon atom (adjacent to $-NH_2$), will attack another aromatic ring, at a *meta*-positioned carbon, in relation to the positively-charged quaternary amino group. This carbon, being in conjugated bonding with the amino group, can become a stable carbocation, while a proton and an electron are transferred to the tertiary amino group, neutralizing it.

In the case of the gold AuQCM substrate, the monomer oxidation peak current increases up to the 5th cycle, meaning that the monomer is being adsorbed. This step is followed by a decrease in the monomer-type set of peaks and the appearance of a second polymer-type set of peaks, which coexist up to the 23rd cycle. After this, the monomer redox activity is no longer detected, and the polymer oxidation current continues to increase up to the 40th cycle and shift towards more positive potential values. The polymer oxidation peak potential shifts by 18 mV towards more positive values, from −0.20 V to −0.02 V *vs.* SCE.

The fact that the polymer oxidation occurs at less negative potentials than that of the monomer, which already has a positive charge on the sulfur heteroatom, means that a smaller amount of energy is needed for this reaction to occur. This can be explained by taking into account that during polymerisation, the amino-group binds to a benzene ring of another monomer, so that the positive charge due to polymer oxidation is more easily delocalized, due to the extended conjugated bonds between monomer moieties. The ability to delocalize the positive charge of the polymer means that a more stable cation is formed, so less energy is required for the oxidation to occur.

At carbon, on the AuQCM/C substrate, the monomer peaks increase only up to the 3rd cycle, up to this cycle MB being adsorbed, and after this polymerisation starts. The peak current attributed to the formation of the radical cation species is more evident at this substrate, and leads to a better polymerisation of MB. The polymer-type set of peaks coexists with the monomer redox response only up to the 12th cycle, after which no monomer response is recorded. Also, the overall increase in polymer oxidation current is twice as high as that recorded at the AuQCM substrate. The oxidation potential shift of 19 mV is very similar to that at the AuQCM without carbon, from −0.18 V to 0.01 V *vs.* SCE.

It can be deduced that AuQCM/C electrodes are better substrates for MB electropolymerisation. This can be due first to better adsorption of the MB monomer on the nano-structured sputtered carbon coating on the Au surface, since the surface becomes rougher and leads to more nucleation sites. Also, carbon is a more hydrophobic substrate than gold, so that adsorption of the phenazine monomer is facilitated. As already mentioned above, when the phenazine monomer has two tertiary amino groups as in MB the cation radicals are formed at very positive potentials, close to +1.0 V *vs.* SCE, which are considered too high for Au electrodes, since formation of gold oxide and oxygen production already occurs around this potential and may limit cation radical formation. The carbon sputtering of the surface overcomes this problem, irreversible oxidation being more pronounced in this case.

The gravimetric monitoring of the deposition processes also exhibits differences. Fig. 5 shows the frequency shift with time recorded during PMB polymer deposition at the two different substrates, where the initial frequency, recorded at the beginning of the potential cycling, is taken as zero. A greater total shift in frequency of ∼−1.33 kHz in the case of the AuQCM/C substrate indicates the deposition of more polymer and a thicker film than at AuQCM electrodes, for which a value of Δf of −0.97 kHz was recorded.

The frequency–time plot during MB electropolymerisation at AuQCM/C can be divided into three parts. The first, up to 5 cycles, is characterized by a shift in frequency of only 55 Hz, or 11 Hz per cycle. The second, from the 6th up to the 18th cycle, shows a higher Δf per cycle of 21 Hz. The highest change in frequency of 55 Hz per cycle occurs from cycle 18 to cycle 30, which means that the highest mass of polymer is deposited in this third step. The overall shift in frequency recorded at the AuQCM/C electrode during MB polymerisation of 1.33 kHz, corresponds to a deposited polymer mass of 16 μg cm^{-2}. Also at AuQCM, the first 15 cycles are characterized by a smaller shift in frequency than the last 25 cycles, when a higher mass of polymer per cycle is deposited.

For both substrate surfaces, the first part of the deposition process is attributed to monomer adsorption and the last with just polymer growth. Probably during the second part, desorption of monomer/oligomers occurs simultaneously with polymer formation, explaining the lower frequency shift compared with the third and last part. Analysis of the individual cycle profiles shows that there is a sudden frequency decrease (mass increase) at 0.5 V with a slower increase which

continues until ~0.60 V is reached on the inverse scan in the negative direction. A fast loss of mass is then seen, *i.e.* monomers and oligomers, so that the net gain in mass per cycle corresponds to 11 Hz (equivalent to 38 ng cm^{-2}). The sudden increase in mass at 0.50 V can be attributed to gold oxide formation. This is borne out by the fact that this feature disappears in later cycles when the gold surface is fully covered. Thus, after the 15th cycle only polymer growth, with some oligomer/monomer desorption on negative-going scans, is seen accompanied by a small mass increase at around −0.2 V that can be attributed to cation insertion.

Taking into account that the gravimetric results were obtained during the polymerisation in electrolyte solution, it is difficult to calculate the real mass of deposited polymer, since, due to the polymer porosity, water molecules and oligomers are entrapped inside the film. It is necessary to estimate the deposited mass of polymer, considering that only monomer moieties which are polymerised at the electrode surface, contribute to the total recorded frequency change during the gravimetric studies. The total equivalent mass calculated using the Sauerbrey equation, *i.e.* assuming no viscoelastic effects and that a compact film is formed, is 3.34 μg for PMB films electropolymerised on AuQCM and 4.58 μg for AuQCM/C. Dividing these values by the molar mass of MB monomer, the number of monomer moieties can be estimated, being 6.29×10^{15} and 8.63×10^{15} MB respectively. The geometric area of the AuQCM electrodes is 0.28 cm^2 and this would correspond to film thicknesses of 120 nm and 164 nm if unit density is assumed, see Table 1.

On the other hand, knowing that a molecule of MB monomer occupies a surface area[24] of 1.92×10^{-14} cm^2, complete monolayer coverage of the electrode surface corresponds to $\sim 1.46 \times 10^{13}$ monomers. If the film thickness of a monolayer of polymer (monomer) is equal to the diameter of one monomer (maximum diameter of MB molecule 1.56 nm), polymer film thicknesses would be 630 nm and 982 nm at AuQCM and AuQCM/C respectively; these estimates are almost certainly too high since some closer packing of the monomer units can be expected.

Unfortunately, the stability of the polymer films deposited on both these substrates is not good, due to the weak adhesion of PMB films at solid substrates, which was also observed when PMB was deposited at carbon film electrodes.[16] Stable PMB films could be formed on glassy carbon substrates as reported in ref. 25. Keeping the polymer from direct contact with the solution may be the key to solving this problem, and in the future we intend to develop a separation membrane, which can be deposited on top of the PMB modified electrodes to improve stability. Due to these problems, no CV or EIS characterisation of the PMB-modified electrodes was done. Nevertheless, the differences between different substrates can be clearly shown by using the EQCM.

3.3 Poly(neutral red) deposition on AuQCM and AuQCM-{HA/Mb}$_6$

The monomer NR was electropolymerised on AuQCM and on AuQCM-{HA/Mb}$_6$, AuQCM electrodes modified with the LBL structures of HA and Mb developed in ref. 2 and 3. The objective of this LBL modification was to explore their applicability in the biosensor area, since this very complex structure represents a way in which both the biorecognition element and redox mediator can be immobilized in a highly ordered nanostructure, with close proximity between the redox centre of the protein and the mediator.

The monomer was electropolymerised by potential cycling in the potential range −1.0 to +1.0 V *vs.* SCE, at 50 mV s^{-1}, from a solution containing 1 mM of NR in 0.025 M KPBS + 0.1 M KNO_3, pH 5.5, as in the optimised procedure described in ref. 17. Fig. 1(A) and 3 show the oxidized/reduced forms of the monomer and polymer together with possible polymerisation linkages between monomers.

Cyclic voltammograms recorded during NR electropolymerisation on both substrates are presented in Fig. 6, where differences between the voltammetric profiles of film formation are evident. At AuQCM electrodes, Fig. 6(A), the profile is different to that previously observed at carbon-based electrodes,[16,26,27] where the monomer and the polymer presented the same oxidation potential values, with a small shift of ~0.14 V of the reduction potential towards more negative potentials, while PNR is being formed on carbon substrates.

At AuQCM electrodes, the oxidation and reduction potentials of the monomer are similar to those reported in ref. 16 and 26, being $E_{ox(NR)} = -0.46$ V and $E_{red(NR)} = -0.61$ V *vs.* SCE. During polymer formation, both reduction and oxidation waves shift by ≈14 mV towards more positive potentials, the midpoint potential of the polymer ($E_{m(PNR)}$) being −0.39 V *vs.* SCE, which is more positive than that obtained at carbon film of $E_{m(PNR)} = -0.63$ V *vs.* SCE,[16] and at carbon composite electrodes, $E_{m(PNR)} = -0.54$ V *vs.* SCE.[26]

As in the case of MB, electropolymerisation begins with adsorption of the monomer at the electrode surface and the formation of cation radicals, which in the case of NR are formed at less positive potentials, around +0.8 V *vs.* SCE. It has been found that phenazine dyes with a primary amino group present as a ring substituent, yield a more stable

Table 1 Values of Δf and Δm obtained from the EQCM measurements during MB and NR polymerisation, and estimated number of monomer moieties and polymer film thickness; electrode geometric area 0.28 cm^2

	Δf/kHz	Δm/μg	Number of monomer moieties × 10^{15}/cm^2	Film thickness/nm
PMB				
AuQCM	0.97	3.34	22.5	120
AuQCM/C	1.33	4.58	30.8	164
PNR				
AuQCM	0.91	3.13	23.2	112
AuQCM-{HA/Mb}$_6$	1.15	3.63	27.1	130

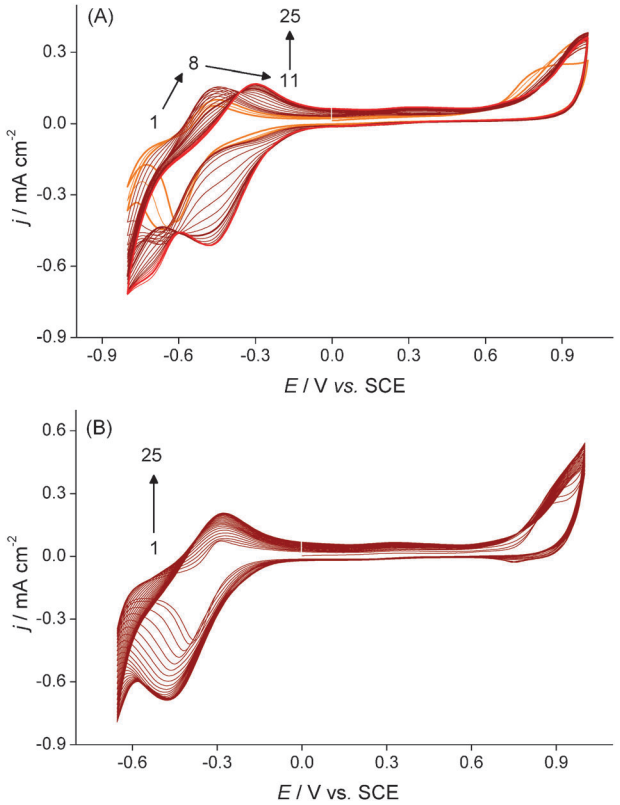

Fig. 6 CVs recorded during the electropolymerisation of NR at (A) AuQCM and (B) AuQCM-{HA/Mb}$_6$ from a solution containing 1 mM NR in 0.025 M KPBS + 0.1 M KNO_3, pH 5.5; v = 50 mV s^{-1}.

singly-charged radical cation upon irreversible oxidation, and thus have a lower energy, a less positive potential being required for the formation of the radical species. The oxidation current due to the monomer increases up to scan 8 and then slightly decreases up to the 11th cycle. At this point the oxidation peak becomes broader, since the polymer peak starts to appear at more positive potentials and coexists with the monomer one. Afterwards, the monomer peak disappears, the polymer peak becoming sharp and better defined at more positive potential values; the current due to the polymer increases up to the last, 25th cycle when it reaches the maximum value.

Fig. 6(B) shows cyclic voltammograms recorded during the deposition of PNR at AuQCM-{HA/Mb}$_6$. In this case, the electropolymerisation profile is more like that observed at carbon-based electrodes, where overlapping of monomer and polymer redox couples occurs. In contrast with phenoxazine and phenothiazines where oxygen and sulfur are the second heteroatom, when both heteroatoms are trivalent nitrogen, monomer and polymer redox activity occurs at the same potentials. This was also observed for NR at other carbon-based substrates[16,20,26,27] and for safranine.[28] The main difference between the two substrates, which can influence NR polymerisation, is the degree of surface non-uniformity, which is more pronounced for the LBL-modified AuQCM (see impedance results in section 3.4.2) and the lamellar structure of the LBL films, so that polymer can also be formed between the layers of HA and Mb. This is very important for application in biosensor construction, since the protein (enzyme) active centre and the redox polymer, being very close to each other, can exchange electrons easily.

Unlike MB, NR monomer has both a trivalent nitrogen heteroatom and a primary amino group ring substituent, so that the positive charge formed during oxidation is already delocalised, even before polymer formation. This explains that the same amount of energy is required for monomer and polymer oxidation and reduction, so that the redox potentials of both have very similar values.

Even though the CV profile recorded during NR polymerisation is similar to those of other carbon-based electrodes, there is a difference in the oxidation–reduction potential values of both monomer and polymer. The redox potentials of the polymer on both AuQCM and AuQCM-{HA/Mb}$_6$ are the same, with $E_{m(PNR)}$ = −0.39 *vs.* SCE, but those of the monomer redox couple differ, as mentioned above.

The overall increase in recorded current, from the first up to the last (25th) cycle, was ≈25% higher than on the unmodified AuQCM electrode, a higher mass of polymer being deposited at this substrate.

Frequency changes recorded at the QCM during the electropolymerisation of NR at AuQCM and AuQCM-{HA/Mb}$_6$ are presented in Fig. 7. The deposition profiles are different: although the change in the frequency variation appears close to continuous, two phases can be identified for the AuQCM substrates and three for the LBL-modified electrode. At the AuQCM substrates the process occurs in 2 steps: first up to the 12th cycle, with Δf = 39 Hz per cycle, and the second one with Δf = 33 Hz per cycle. Compared with PMB the individual frequency changes in each cycle are smaller and the small decrease in frequency associated with cation insertion is visible. There is no evidence of the effect of gold oxide formation in this case. The total deposited mass is 11.0 μg cm^{-2}.

At AuQCM-{HA/Mb}$_6$ substrates, the deposition of PNR is slower during the first cycles, with a shift in frequency of 32 Hz per cycle. A second part, with the highest deposition rate of PNR is recorded up to the 15th cycle, characterized by a frequency shift of 48 Hz per cycle, and the last 10 cycles present a slightly slower deposition rate of PNR (Δf of 41 Hz per cycle) as maximum film deposition is reached.

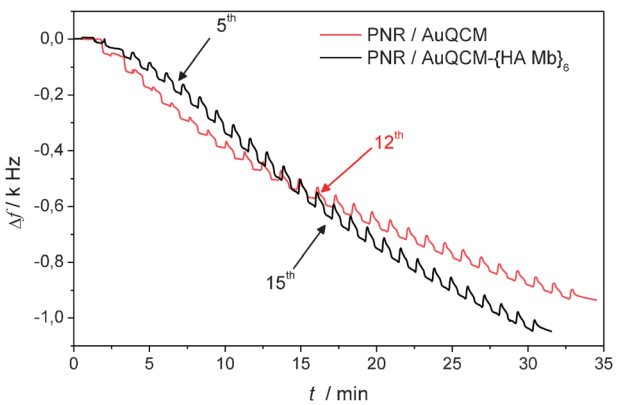

Fig. 7 Frequency shift recorded during the electropolymerisation of NR at AuQCM and AuQCM-{HA/Mb}$_6$ substrates.

The total shift in frequency is −1.10 kHz, corresponding to a deposited polymer mass of 12.9 μg cm^{-2}, higher than that deposited at AuQCM. The individual frequency variations per cycle show the same tendencies as at AuQCM substrates.

The same procedure and model presented for the estimation of polymer PMB thickness and mass was used also in the case of PNR. The total mass corresponding to the overall shift in frequency recorded was 3.13 μg and 3.63 μg PNR, corresponding to 6.50×10^{15} and 7.58×10^{15} NR monomers on AuQCM and for AuQCM-$\{HA/Mb\}_6$ respectively. Knowing that the area occupied by one NR monomer[29] is 1.30×10^{-14} cm^2, it can be deduced that $\sim 2.15 \times 10^{13}$ monomers will cover the electrode surface of 0.28 cm^2. Using the same procedure as for PMB, film thicknesses can be estimated as 112 nm and 130 nm for AuQCM and AuQCM-$\{HA/Mb\}_6$ substrates respectively.

The stability of both AuQCM and AuQCM-$\{HA/Mb\}_6$ was tested in 0.1 M KCl, by recording 100 cyclic voltammograms at 100 mV s^{-1} scan rate. The PNR/AuQCM electrode showed a very small variation in the recorded current from the first to the last cycle (a constant decrease in current of ≈10% from the 1st to the 100th cycle), meaning that the modified electrode is stable. In the case of the PNR/LBL modified AuQCM, there is a slight decrease in current during the first 10 cycles, probably correlated with the desorption of entrapped oligomers.

3.4 Electrochemical characterisation of PNR-modified AuQCM and AuQCM-$\{HA/Mb\}_6$ electrodes

3.4.1 Cyclic voltammetry. PNR-modified electrodes were characterised by cyclic voltammetry in 0.1 M KCl. Both PNR/AuQCM and PNR/AuQCM-$\{HA/Mb\}_6$ showed a linear dependence of peak current on square root of the scan rate (see Fig. 8(A) and (B)), indicating that the overall electrochemical process is diffusion controlled. As already described in ref. 16, for phenazine-modified electrodes the diffusion dependence is attributed to the rate-limiting diffusion of counterions through the polymer network in order to maintain the electroneutrality during the redox reaction which occurs at the electrode. As observed from Fig. 8(B), in the case of PNR/AuQCM-$\{HA/Mb\}_6$ electrodes, the peaks are not as well-defined as in the case of PNR/AuQCM, and this can be explained by taking into account the complex structure of the substrate assembly, constituted by 6 bilayers of HA and Mb deposited on a precursor-modified AuQCM electrode. Since this assembly has some non-uniformity and molecule-sized channels it can be expected that some of the PNR is formed within the top of the multilayer structure.

Examination of the cyclic voltammograms shows that the slope of the plot of anodic peak current *versus* $v^{1/2}$ is smaller, being 15 μA cm^{-2} (mV s^{-1})$^{-1/2}$ at PNR/AuQCM-$\{HA/Mb\}_6$ compared with 25 μA cm^{-2} (mV s^{-1})$^{-1/2}$, for the PNR/AuQCM electrode. Additionally, the anodic current does not increase in value above a sweep rate of 75 mV s^{-1}, which can be ascribed to diffusion barriers for counterion insertion into the PNR/LBL structure. For the cathodic process, expulsion of the counterions involved in the redox process occurs faster for the PNR/AuQCM-$\{HA/Mb\}_6$, being reflected in the slope of 44, higher than 26 μA cm^{-2} (mV s^{-1})$^{-1/2}$ at the PNR/AuQCM electrode. Insertion of the counterion is probably more difficult than its expulsion due to the fact that when inserted the ion brings solvent molecules with it whereas when it leaves the film it does not, so that the volume is much smaller, allowing easier diffusion.

3.4.2 Electrochemical impedance spectroscopy (EIS). Electrochemical impedance spectroscopy was used to examine the interfacial properties of the unmodified AuQCM electrode and the PNR-modified AuQCM and AuQCM-$\{HA/Mb\}_6$ electrodes in 0.1 M KCl at potentials equal to the open circuit potential (OCP), measured before each experiment and which was found to be ∼ +0.27 and ∼ +0.14 V *vs.* SCE for the PNR/AuQCM and PNR/AuQCM-$\{HA/Mb\}_6$ electrodes respectively. Two other, more negative, applied potentials were also used, −0.35 and −0.48 V *vs.* SCE, in the region where the polymer redox reactions occur.

Spectra recorded at an unmodified AuQCM electrode in 0.1 M KCl at OCP (∼0.07 V *vs.* SCE) and at −0.35 V *vs.* SCE, in order to have a comparison so as to better evaluate how PNR and PNR/LBL influence the charge transfer at the electrode interface, are shown in Fig. 9(A). As can be seen, at OCP the impedance values are very high whereas at −0.35 V *vs.* SCE, closer to the hydrogen evolution potential, there is a substantial decrease in the values.

Complex plane impedance spectra recorded at PNR-modified electrodes are illustrated in Fig. 9(B) and (C). Modification by PNR leads to a substantial decrease of the impedance values at all potentials investigated. The impedance values are lower at −0.35 and −0.48 V *vs.* SCE, due to the fact that, in this potential region, oxidation and reduction of the polymer occurs. There is a lack of consistency with the diffusion-controlled behaviour seen by cyclic voltammetry, although the curving upwards of the spectra at low frequency at the PNR-modified electrodes, at the potentials where the PNR redox couple occurs, is possible evidence of some influence of diffusion control.

The higher frequency semicircular part impedance spectra were fitted by an electrical equivalent circuit which consists of a cell resistance, R_Ω, in series with a combination of a charge transfer resistance, R_{ct}, in parallel with a constant phase element modeled as a non-ideal capacitor, given by CPE = $((i\omega C)^{\alpha})^{-1}$, where C is the capacitance, ω is the frequency in rad s^{-1} and the exponent α reflects the surface non-uniformity and polymer film porosity, having a maximum value of 1.0 and minimum of 0.5. The α exponent for the unmodified AuQCM electrode had the highest value of 0.85, whereas values of 0.73 and 0.68 were found for the PNR/AuQCM and PNR/AuQCM-$\{HA/Mb\}_6$ electrodes respectively. The fact that the mean roughness, R_a, presented in the AFM section, has the lowest value for the LBL-modified AuQCM whereas the lowest α value of these substrates clearly indicates a higher non-uniformity of the PNR-modified electrodes, as also reported in ref. 3.

The resistance and capacitance values obtained by fitting the impedance spectra with the equivalent circuit are presented in Table 2. As observed, the more negative the applied potential, the lower the charge transfer resistance, since the midpoint potential of the PNR is being approached. The unmodified AuQCM electrode has a R_{ct} at OCP of 56.0 kΩ cm^2, and the

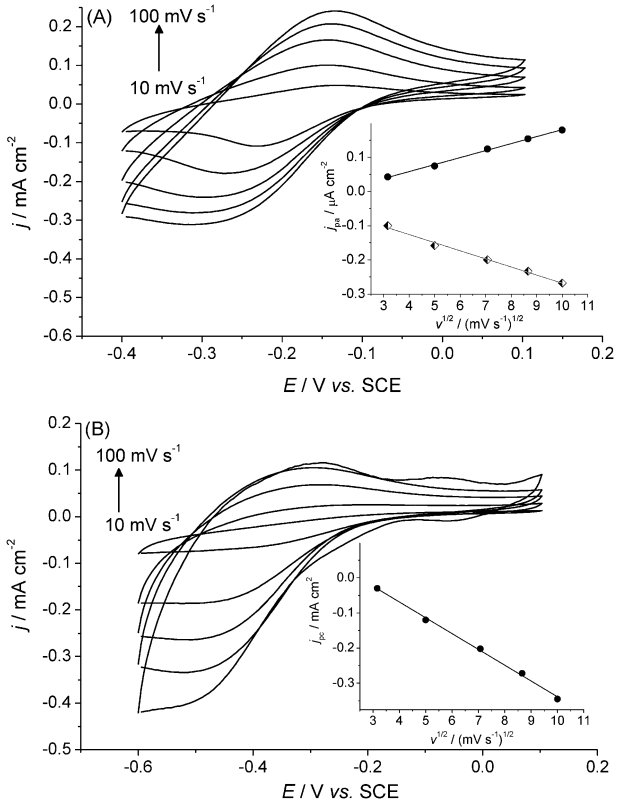

Fig. 8 Cyclic voltammograms recorded at (A) PNR/AuQCM and (B) PNR/AuQCM-{HA/Mb}$_6$ modified electrodes in 0.1 M KCl at scan rates from 10 to 100 mV s^{-1}.

PNR modified ones have lower R_{ct} values of 4.7 and 6.9 kΩ cm^2 for PNR/AuQCM and PNR/AuQCM-{HA/Mb}$_6$ electrodes respectively. At −0.35 V *vs.* SCE, between the PNR-modified electrodes, the less resistive is the PNR/AuQCM-{HA/Mb}$_6$ with 3.9 kΩ cm^2. At this potential the unmodified AuQCM electrode also has a small value of R_{ct}, due to the proximity to the hydrogen evolution potential. At −0.48 V *vs.* SCE, both PNR-modified electrodes present the same charge transfer resistance of 5.8 kΩ cm^2.

The largest interfacial capacitance values were recorded at −0.48 V *vs.* SCE for both modified electrodes, being of 170 and 143 μF cm^{-2} s$^{\alpha-1}$, highest for the PNR/AuQCM electrode. This can be attributed to the dielectric constant values of PNR films being greater than those of PNR/LBL films.

4. Conclusions

The phenazine monomers methylene blue (MB) and neutral red (NR) have been successfully electropolymerised: MB on AuQCM and AuQCM/C and NR on AuQCM and on AuQCM-{HA/Mb}$_6$. The electropolymerisation process occurs in a different way due to the difference in the monomer chemical structure, and is strongly influenced by the electrode substrate as demonstrated by AFM, voltammetry and microbalance gravimetric measurements. The monomer MB electropolymerises better on AuQCM/C, reflected in a higher current increase and greater deposited mass. This is due to the larger potential window of these electrodes, which enables

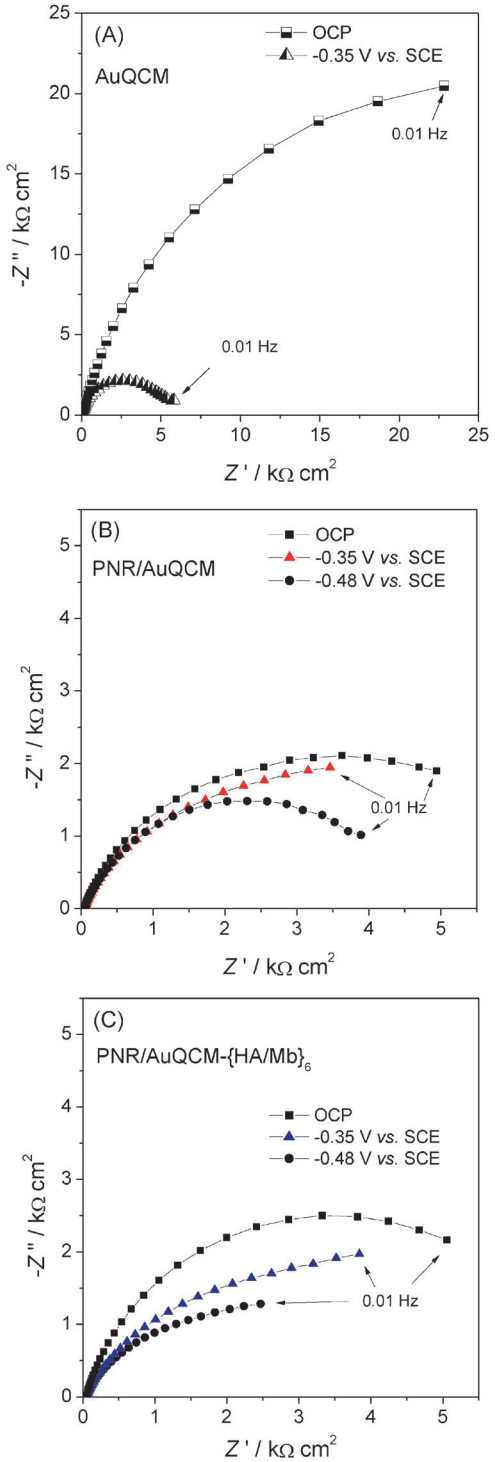

Fig. 9 Impedance spectra recorded at (A) AuQCM (B) PNR/AuQCM and (C) PNR/AuQCM-{HA/Mb}$_6$ electrodes in 0.1 M KCl.

a better formation of the cation radical at positive potentials, responsible for the initiation of the polymerisation process, as well as to the more pronounced hydrophobic character of carbon compared with gold substrates, which plays an important role in monomer adsorption. This demonstrates the importance of the recently developed gold-coated QCM electrodes covered with ultrathin nanostructured sputtered carbon films, for investigating electrochemical processes.

Table 2 Resistance and capacitance values obtained by fitting the high frequency part of the impedance spectra with the equivalent circuit described in the text

	Electrode type					
	AuQCM		PNR/AuQCM		PNR/AuQCM-{HA/Mb}$_6$	
E/V *vs.* SCE	C_{dl}/μF cm^{-2} s$^{\alpha-1}$	R_{ct}/kΩ cm^2	C_{dl}/μF cm^{-2} s$^{\alpha-1}$	R_{ct}/kΩ cm^2	C_{dl}/μF cm^{-2} s$^{\alpha-1}$	R_{ct}/kΩ cm^2
OCP	35.0	56.0	97.1	4.7	106.0	6.9
–0.35	27.1	5.5	90.2	6.3	24.1	3.9
–0.48	—	—	170.0	5.8	143.3	5.8

The monomer NR electropolymerises better than MB on AuQCM and the polymer film is more stable, due to higher monomer hydrophobicity. The AuQCM-{HA/Mb}$_6$ substrate led to better polymerisation of NR than on the unmodified AuQCM. The properties of the PNR-modified electrodes were investigated by cyclic voltammetry and by electrochemical impedance spectroscopy. The polymer redox process shows diffusion control for both types of modified electrode and the charge transfer at PNR/AuQCM-{HA/Mb}$_6$ electrodes is easier than for PNR/AuQCM.

Both ultrathin nanostructured graphite and layer-by-layer deposited multilayer films of HA/Mb improved the electrochemical properties of phenazine polymers formed on AuQCM electrode substrates, and thence for application as polymer-modified electrodes in electrochemical sensors and in redox-mediated biosensors.

Acknowledgements

Financial support from Fundação para a Ciência e a Tecnologia (FCT), PTDC/QUI/65255/2006 and PTDC/QUI/65732/2006, POCI 2010 (co-financed by the European Community Fund FEDER) and CEMUC® (Research Unit 285), Portugal, is gratefully acknowledged. MMB and EMP thank FCT for PhD grants SFRH/BD/27864/2006 and SFRH/BD/31483/2006 respectively.

References

1 E. M. Pinto, C. Gouveia-Caridade, D. M. Soares and C. M. A. Brett, *Appl. Surf. Sci.*, 2009, **255**, 8084.
2 M. M. Barsan, E. M. Pinto and C. M. A. Brett, *Electrochim. Acta*, 2010, **55**, 6358.
3 E. M. Pinto, M. M. Barsan and C. M. A. Brett, *J. Phys. Chem. B*, 2010, **114**, 15354.
4 R. Pauliukaite, M. E. Ghica, M. M. Barsan and C. M. A. Brett, *Anal. Lett.*, 2010, **43**, 1588.
5 R. Pauliukaite, M. E. Ghica, M. M. Barsan and C. M. A. Brett, *J. Solid State Electrochem.*, 2007, **11**, 899.
6 D. M. Zhou, H. Q. Fang, H. Y. Chen, H. X. Ju and Y. Wang, *Anal. Chim. Acta*, 1996, **329**, 41.
7 Y. V. Ulyanova, A. E. Blackwell and S. D. Minteer, *Analyst*, 2006, **131**, 257.
8 R. Yang, C. Ruan and J. Deng, *J. Appl. Electrochem.*, 1998, **28**, 1269.
9 W. J. Albery, A. W. Foulds, K. J. Hall and A. R. Hillman, *J. Electrochem. Soc.*, 1980, **127**, 654.
10 W. J. Albery, M. G. Boutelle and A. R. Hillman, *J. Electroanal. Chem.*, 1985, **182**, 99.
11 D. Benito, C. Gabrielli, J. J. García-Jareño, M. Keddam, H. Perrot and F. Vicente, *Electrochem. Commun.*, 2002, **4**, 613.
12 J. Clavilier, V. Svetlicic, V. Zutic, B. Ruacic and J. Chevalet, *J. Electroanal. Chem.*, 1988, **250**, 427.
13 V. Svetlicie, V. Zutie, J. Clavilier and J. Chevalet, *J. Electroanal. Chem.*, 1987, **233**, 199.
14 V. Zutie, V. Svetlicic, J. Clavilier and J. Chevalet, *J. Electroanal. Chem.*, 1987, **219**, 183.
15 V. Kertész, J. Bácskai and G. Inzelt, *Electrochim. Acta*, 1996, **41**, 2877.
16 M. M. Barsan, E. M. Pinto and C. M. A. Brett, *Electrochim. Acta*, 2008, **53**, 3973.
17 M. E. Ghica and C. M. A. Brett, *Electroanalysis*, 2006, **18**, 748.
18 G. Sauerbrey, *Z. Phys.*, 1959, **155**, 206.
19 E. S. Gadelmawla, M. M. Koura, T. M. A. Maksoud, I. M. Elewa and H. H. Soliman, *J. Mater. Process. Technol.*, 2002, **123**, 133.
20 A. A. Karyakin, E. E. Karyakina and H.-L. Schmidt, *Electroanalysis*, 1999, **11**, 149.
21 D. D. Schlereth and A. A. Karyakin, *J. Electroanal. Chem.*, 1995, **395**, 221.
22 M. E. Ghica and C. M. A. Brett, *J. Electroanal. Chem.*, 2009, **629**, 35.
23 A. Malinauskas, G. Niaura, S. Bloxham, T. Ruzgas and L. Gorton, *J. Colloid Interface Sci.*, 2000, **230**, 122.
24 C. Kaewprasit, E. Hequet, N. Abidi and J. P. Gourlot, *J. Cotton Sci.*, 1998, **2**, 164.
25 C. M. A. Brett, G. Inzelt and V. Kertész, *Anal. Chim. Acta*, 1999, **385**, 119.
26 M. M. Barsan, E. M. Pinto, M. Florescu and C. M. A. Brett, *Anal. Chim. Acta*, 2009, **635**, 71.
27 R. C. Carvalho, C. Gouveia-Caridade and C. M. A. Brett, *Anal. Bioanal. Chem.*, 2010, **398**, 1675.
28 R. Pauliukaite, A. Selskiene, A. Malinauskas and C. M. A. Brett, *Thin Solid Films*, 2009, **517**, 5435.
29 C. Chen and Y. Gao, *Russ. J. Electrochem.*, 2007, **43**, 267.